

Rethinking Sparse Gaussian Processes: Bayesian Approaches to Inducing-Variable Approximations

Simone Rossi¹ Markus Heinonen² Edwin Bonilla³ Zheyang Shen² Maurizio Filippone¹

Abstract

Variational inference techniques based on inducing variables provide an elegant framework for scalable posterior estimation in Gaussian process (GP) models. Most previous works treat the locations of the inducing variables, i.e. the inducing inputs, as variational hyperparameters, and these are then optimized together with GP covariance hyper-parameters. While some approaches point to the benefits of a Bayesian treatment of GP hyper-parameters, this has been largely overlooked for the inducing inputs. In this work, we show that treating both inducing locations and GP hyper-parameters in a Bayesian way, by inferring their full posterior, further significantly improves performance. Based on stochastic gradient Hamiltonian Monte Carlo, we develop a fully Bayesian approach to scalable GP and deep GP models, and demonstrate its competitive performance through an extensive experimental campaign across several regression and classification problems.

1. Introduction and Motivation

Bayesian kernel machines based on Gaussian process (GPs) offer the modeling flexibility of kernel methods combined with the ability to characterize the uncertainty in predictions and model parameters (Rasmussen & Williams, 2006). The field of GPs has considerably evolved in the last few years with key contributions in modeling and inference in the direction of making GPs scalable to virtually any number of data points, using mini-batches, and suitable for implementations in languages featuring automatic differentiation (Matthews et al., 2017; Krauth et al., 2017), thus making them easy to implement and use. This has been possible thanks to the combination of variational inference techniques with popular GP approximations, such as induc-

Table 1: A comparison of inference methods for GP models. θ , \mathbf{U} , \mathbf{Z} refer to the GP latent function values, covariance hyper-parameters, inducing variables and inducing inputs, respectively. Notably, the variational methods do not infer exact posteriors.

Model	Exact inference			Reference
	θ	\mathbf{u}	\mathbf{Z}	
MCMC-GP	✓	-	-	Neal (1997); Barber & Williams (1997)
SVGP	✗	✗	✗	Hensman et al. (2015a)
SGHMC-DGP	✗	✓	✗	Havasi et al. (2018b)
IPVI-DGP	✗	✓	✗	Yu et al. (2019)
MCMC-SVGP	✓	✓	✗	Hensman et al. (2015b)
BSGP	✓	✓	✓	this work

ing points (Titsias, 2009; Lázaro-Gredilla & Figueiras-Vidal, 2009; Hensman et al., 2013), random features (Rahimi & Recht, 2008; Cutajar et al., 2017; Gal & Ghahramani, 2016), and structured approximations (Wilson & Nickisch, 2015; Wilson et al., 2016b). These advancements have now put GPs in the position to be attractive models for a variety of applications using a variety of likelihoods (Matthews et al., 2017; Bonilla et al., 2019).

In this work, we focus in particular on variationally sparse GPs as originally formulated by Titsias (2009) and later developed by Hensman et al. (2013) to scale up to very large datasets via stochastic (mini-batch) optimization. In these formulations, the GP prior is augmented with inducing variables (drawn from the same prior) and their posterior is estimated via variational inference. In contrast, the locations of the inducing variables, which we refer to as the inducing inputs, are only optimized along with covariance hyper-parameters. In line with previous evidence that a fully Bayesian treatment of GPs is beneficial for performance of GP models (Neal, 1997; Barber & Williams, 1997; Murray & Adams, 2010; Filippone & Girolami, 2014), following up on the works on variational sparse GPs, there have been studies showing that full posterior inference of the inducing variables jointly with covariance hyper-parameters improves performance (Hensman et al., 2015b).

Despite these significant insights, the common practice in GP models to date is to only carry out point estimation of the inducing inputs, usually via continuous optimization. In fact, the original work of Titsias (2009) advocates for the

¹Data Science Department, EURECOM, France ²Department of Computer Science, Aalto University, Finland ³CSIROs Data61, Australia. Correspondence to: Simone Rossi <simone.rossi@eurecom.fr>.

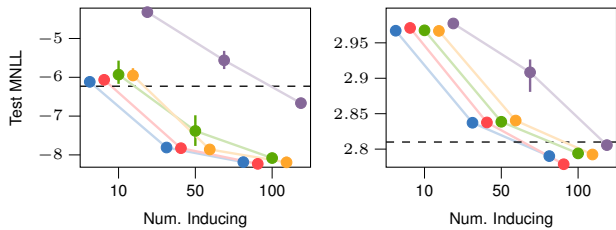


Figure 1: Comparison of test mean negative loglikelihood (MNLL) on NAVAL (left) and PROTEIN (right) for different number of inducing variables and for determinantal point process prior (●), normal prior (●), Strauss process prior (●) and uniform prior (●). Finally, (●) corresponds to the case of inducing points optimized and covariance hyper-parameters inferred similarly to Hensman et al. (2015a), while (- -) is the performance reached by SGHMC-DGP with 100 points from Havasi et al. (2018b).

treatment of the inducing inputs as variational parameters, arguing that under the proposed framework their optimization should be protected from overfitting. Furthermore, later work concludes that point estimation of the inducing inputs through optimization of the variational objective is an ‘optimal’ treatment (Hensman et al., 2015b, §3). We believe that the conceptual justification for inducing-input optimization in this latter work deserves some consideration, as it relies on being able to optimize both the prior and the posterior. To the best of our knowledge, even the most recent developments in GP inference still carry out point estimation of the inducing inputs (Havasi et al., 2018b; Shi et al., 2019). We summarise the inference differences of the current methods in Table 1.

In this paper, we aim to rethink the role of the inducing inputs in GP models and their treatment as variational parameters or even hyper-parameters. Given their potential high dimensionality and that the typical number of inducing variables go beyond hundreds and even thousands (Shi et al., 2019), we argue that they should be treated simply as model variables and, therefore, having priors and carrying efficient posterior inference over them is an important – although challenging – problem.

Our contribution is to demonstrate that a fully Bayesian treatment of the inducing inputs is possible thanks to recent advances in stochastic gradient-based Markov chain Monte Carlo sampling (Chen et al., 2014; Havasi et al., 2018b) and that this leads to improved performance compared to alternatives where the inducing inputs are optimized. We study the effect of the Bayesian treatment of inducing inputs by analyzing the effect on the distribution of the covariance function and in light of the ensembling effect in predictions, which allows for a richer modeling capability without the need to increase the number of inducing variables. Our experiments show such improvements across a wide range of benchmark and large-scale datasets, as well as for a variety

of GP models, including Deep GPs.

Figure 1 shows a preview of such results. By jointly inferring a free-form posterior on covariance hyper-parameters, inducing variables and inducing inputs one can considerably improve GP inference over state-of-the-art methods.

2. Preliminaries and Related Works

A GP defines a distribution over functions $f : \mathbb{R}^D \rightarrow \mathbb{R}$, for which any finite marginal follows a Gaussian distribution (Rasmussen & Williams, 2005). A GP is fully described by a mean function $m(\mathbf{x})$ and a covariance function $k(\mathbf{x}, \mathbf{x}'; \boldsymbol{\theta})$ with hyper-parameters $\boldsymbol{\theta}$. Given a supervised learning problem with N pairs of inputs \mathbf{x}_i and labels y_i , $\mathcal{D} = \{(\mathbf{x}_i, y_i) | \mathbf{x}_i \in \mathbb{R}^D, y_i \in \mathbb{R}\}_{i=1, \dots, N}$, we consider a GP prior over functions which are fed to a suitable likelihood function to model the observed labels.

Denoting by $\mathbf{f} \in \mathbb{R}^N$ the realizations of the GP random variables at the N inputs $\mathbf{X} = \{\mathbf{x}_1, \dots, \mathbf{x}_N\}$ and assuming a zero-mean GP prior, we have that $p(\mathbf{f}) = \mathcal{N}(\mathbf{0}, \mathbf{K}_{\mathbf{xx}} | \boldsymbol{\theta})$, where $\mathbf{K}_{\mathbf{xx}} | \boldsymbol{\theta}$ is the covariance matrix obtained by evaluating $k(\mathbf{x}, \mathbf{x}'; \boldsymbol{\theta})$ over all input pairs $\mathbf{x}_i, \mathbf{x}_j$ (we will drop the explicit parameterization on $\boldsymbol{\theta}$ to keep the notation uncluttered). In the Bayesian setting, given a suitable likelihood function $p(\mathbf{y} | \mathbf{f})$, the objective is to characterize the posterior $p(\mathbf{f} | \mathbf{y})$ given N pairs of inputs and labels (see Figure 2a). This inference problem is analytically tractable only in the case of a Gaussian likelihood $\mathbf{y} | \mathbf{f} \sim \mathcal{N}(\mathbf{f}, \sigma^2 \mathbf{I})$, but it involves the costly $\mathcal{O}(N^3)$ inversion of the covariance matrix $\mathbf{K}_{\mathbf{xx}}$.

Sparse GPs are a family of approximate models that address the scalability issue by introducing a set of M inducing variables $\mathbf{u} = (u_1, \dots, u_M)$ at corresponding inducing inputs $\mathbf{Z} = \{\mathbf{z}_1, \dots, \mathbf{z}_M\}$ such that $u = f(\mathbf{z})$ (Snelson & Ghahramani, 2005). These inducing variables are assumed to be drawn from the same GP as the original process, yielding the joint prior $p(\mathbf{f}, \mathbf{u}) = p(\mathbf{u})p(\mathbf{f} | \mathbf{u})$ with

$$\begin{aligned} p(\mathbf{u}) &= \mathcal{N}(\mathbf{0}, \mathbf{K}_{\mathbf{zz}}) \\ p(\mathbf{f} | \mathbf{u}) &= \mathcal{N}(\mathbf{K}_{\mathbf{xz}} \mathbf{K}_{\mathbf{zz}}^{-1} \mathbf{u}, \mathbf{K}_{\mathbf{xx}} - \mathbf{K}_{\mathbf{xz}} \mathbf{K}_{\mathbf{zz}}^{-1} \mathbf{K}_{\mathbf{zx}}), \end{aligned} \quad (1)$$

where $\mathbf{K}_{\mathbf{zz}} \equiv k(\mathbf{Z}, \mathbf{Z})$, $\mathbf{K}_{\mathbf{xz}} \equiv k(\mathbf{X}, \mathbf{Z})$ and $\mathbf{K}_{\mathbf{zx}} = \mathbf{K}_{\mathbf{xz}}^T$ (see Figure 2b). After introducing the inducing variables, the interest is in obtaining a posterior distribution over \mathbf{f} by relying on the set of inducing variables \mathbf{u} so as to avoid costly algebraic operations with $\mathbf{K}_{\mathbf{xx}} \in \mathbb{R}^{N \times N}$. A general framework to do this for any likelihood and at scale (using mini-batches) can be obtained using variational inference techniques (Titsias, 2009; Hensman et al., 2013; Bonilla et al., 2019). The main innovation in Titsias (2009) is the formulation of an approximate posterior $q(\mathbf{f}, \mathbf{u})$ within variational inference (Jordan et al., 1999) so as to develop such a framework. This variational distribution formulation has

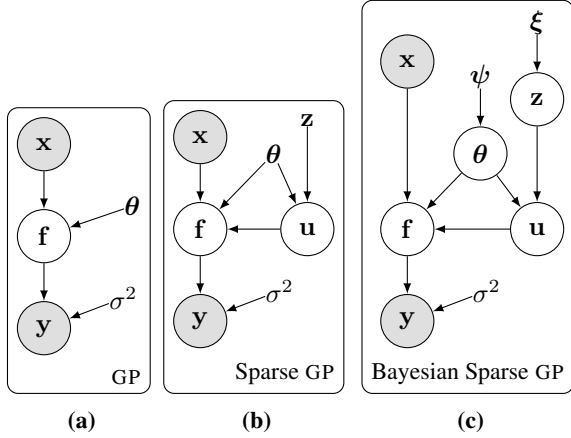


Figure 2: The graphical models of vanilla GPs (a), sparse GPs (b), and the proposed Bayesian sparse GPs (c) with priors on hyperparameters θ , inducing inputs \mathbf{Z} and outputs \mathbf{u} .

come to be known as Titsias’ trick and has the form:

$$q(\mathbf{f}, \mathbf{u}) = q(\mathbf{u})p(\mathbf{f}|\mathbf{u}). \quad (2)$$

Following the variational inference approach, and using the above approximate posterior, we introduce the evidence lower bound (ELBO),

$$\log p(\mathbf{y}) \geq -\text{KL}[q(\mathbf{u}) \parallel p(\mathbf{u})] + \mathbb{E}_{q(\mathbf{f}, \mathbf{u})} \log p(\mathbf{y} | \mathbf{f}), \quad (3)$$

where the Kullback-Leibler divergence (KL) term only involves M -dimensional distributions, as the exact conditional prior (Equation 1) is also used in the approximate posterior (Equation 2), which results in the KL involving N -dimensional distributions vanish. The second term in the expression above is usually referred to as the expected log likelihood (ELL) and, for factorized conditional likelihoods, it can be computed efficiently using quadrature or Monte Carlo (MC) sampling (Hensman et al., 2015a; Bonilla et al., 2019). Thus, posterior estimation under this framework involves constraining $q(\mathbf{u})$ to have a parametric form (usually a Gaussian) and finding its parameters so as to optimize the ELBO above. This optimization can be carried out using stochastic-gradient methods operating on mini-batches yielding a time complexity of $O(M^3)$.

2.1. MCMC for Variationally Sparse GPs

An alternative treatment of the inducing variables under the variational framework described above is to avoid constraining $q(\mathbf{u})$ to having any parametric form or admitting simplistic factorizing assumptions. As shown by Hensman et al. (2015b), this can be, in fact, achieved by finding the optimal (unconstrained) distribution $q(\mathbf{u})$ that maximizes the ELBO in Equation 3 and sampling from it using techniques such as Markov chain Monte Carlo (MCMC). This

optimal distribution can be shown to have the form

$$\log q(\mathbf{u}) = \mathbb{E}_{p(\mathbf{f}|\mathbf{u})} \log p(\mathbf{y}|\mathbf{f}) + \log p(\mathbf{u}) + C, \quad (4)$$

where C is an unknown normalizing constant. This expression makes it apparent that sparse variational GPs can be seen as GP models with a Gaussian prior over the inducing variables and a likelihood which has a complicated form due to the expectation under the conditional $p(\mathbf{f}|\mathbf{u})$. This observation makes it possible to derive MCMC samplers for the posterior over \mathbf{u} , thus relaxing the constraint of having to deal with a fixed form approximation. The only difficulty is that the likelihood requires the computation of an expectation; however, as mentioned above, for most modeling problems where the likelihood factorizes, this expectation can be calculated as a sum of univariate integrals, for which it is easy to employ numerical quadrature.

Hensman et al. (2015b) also include the sampling of the hyper-parameters θ jointly with \mathbf{u} ; however, in order to do this efficiently, a whitening representation is employed, whereby the inducing variables are reparameterized as $\mathbf{u} = \mathbf{L}_{zz}\boldsymbol{\nu}$, with $\mathbf{K}_{zz} = \mathbf{L}_{zz}\mathbf{L}_{zz}^\top$. The sampling scheme then amounts to sampling from the joint posterior over $\boldsymbol{\nu}, \theta$.

The actual sampling scheme proposed by Hensman et al. (2015b) employs a more efficient method based on Hamiltonian Monte Carlo (HMC, Duane et al., 1987; Neal, 2010). Given a potential energy function defined as $U(\mathbf{u}) = -\log p(\mathbf{u}, \mathbf{y}) = -\log p(\mathbf{u}|\mathbf{y}) + C$, Hamiltonian Monte Carlo (HMC) introduces auxiliary momentum variables \mathbf{r} and it generates samples from the joint distribution $p(\mathbf{u}, \mathbf{r})$ by simulation of the Hamiltonian dynamics

$$\begin{aligned} d\mathbf{u} &= \mathbf{M}^{-1}\mathbf{r}dt, \\ d\mathbf{r} &= -\nabla U(\mathbf{u})dt, \end{aligned}$$

where \mathbf{M} is the so called mass matrix, followed by a Metropolis accept/reject step.

2.2. Stochastic gradient HMC for Deep models

Different from classic HMC where it is required to compute the full gradients $\nabla U(\mathbf{u}) = -\nabla \log p(\mathbf{u}|\mathbf{y})$, Stochastic Gradient Hamiltonian Monte Carlo (SGHMC) (Chen et al., 2014) allows to sample from the true intractable posterior by means of stochastic gradients, and without the need of Metropolis accept/reject steps, which would require access to the whole data set. By modeling the stochastic gradient noise as normally distributed $\mathcal{N}(\mathbf{0}, \mathbf{V})$, the (discretized) Hamiltonian dynamics are updated as follows

$$\begin{aligned} \mathbf{u}_{t+1} &= \mathbf{u}_t + \varepsilon \mathbf{M}^{-1}\mathbf{r}_t, \\ \mathbf{r}_{t+1} &= \mathbf{r}_t - \varepsilon \widetilde{\nabla U}(\mathbf{u}) - \varepsilon \mathbf{C}\mathbf{M}^{-1}\mathbf{r}_t + \mathcal{N}(\mathbf{0}, 2\varepsilon(\mathbf{C} - \widetilde{\mathbf{B}})), \end{aligned}$$

where ε is the step size, \mathbf{C} is a user defined friction term and $\widetilde{\mathbf{B}}$ is the estimated diffusion matrix of the gradient noise; see

e.g., [Springenberg et al. \(2016\)](#) for ideas on how to estimate these parameters.

A similar approach can be adopted for deep Gaussian processes (DGPs) ([Damianou & Lawrence, 2013](#)). A DGP is a model obtained by composing layers parameterized by GPs. Each layer is associated with a set of inducing inputs $\{\mathbf{Z}_l\}_{l=1}^L$ and a set of inducing variables $\{\mathbf{U}_l\}_{l=1}^L$ ([Salimbeni & Deisenroth, 2017](#)). SGHMC is the primary inference method used by [Havasi et al. \(2018a\)](#) for obtaining samples from the posterior distribution over the latent variables at all layers $\{\mathbf{U}_l\}_{l=1}^L$. Recently, this has been approached using adversarial inference methods ([Yu et al., 2019](#)).

2.3. Other Approaches to Scalable and Bayesian GPs

It is worth mentioning that, as mentioned in [section 1](#), other approaches to scalable inference in GPs have been proposed, which feature the possibility to operate using mini-batches. For example, looking at the feature-space view of kernel machines, [Rahimi & Recht \(2008\)](#) show how random features can be obtained for shift invariant covariance functions, like the commonly used squared exponential. These approximations are also useful for addressing the scalability of GPs and DGPs, as showed by [Lázaro-Gredilla et al. \(2010\)](#) and [Cutajar et al. \(2017\)](#). Similarly, the work on structured approximations of GPs ([Saatçi, 2011](#)) has found applications to develop a scalable framework for GPs, later developed to include the possibility to learn deep learning-based representations for the input ([Wilson et al., 2016b](#)).

The Gaussian process latent variable model (GPLVM) proposed by [Lawrence \(2005\)](#) is a popular approach to Bayesian nonlinear dimensionality reduction and its Bayesian extensions such as those developed by [Titsias & Lawrence \(2010\)](#) consider a prior over the inputs of a GP. Although these methods can be used for training GPs with missing or uncertain inputs, we are not aware of previous work adopting such methodologies for inducing inputs within scalable sparse GP models.

3. Fully Bayesian Sparse Deep Gaussian Process

In this section, we question the common practice of treating inducing inputs as variational parameters, and propose our Bayesian Sparse Gaussian Process (BSGP) framework, where we carry out full posterior estimation of these variables.

While GPs are advocated as fully probabilistic models, it is common practice to treat covariance hyper-parameters and inducing inputs through optimization, which somewhat goes against this philosophy. We argue that in the spirit of Bayesian modeling, any uncertainty in the covariance should be accounted for.

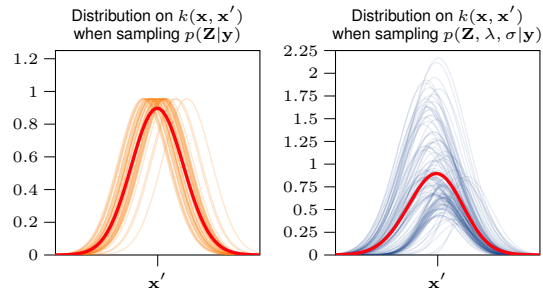


Figure 3: Representation of the posterior induced distribution on the covariance function computed at location \mathbf{x}' .

Thinking of GP hyper-parameters and inducing inputs as parameters of the covariance function, a distribution over these induces a distribution over the covariance function, which enriches the modeling capabilities of these models ([Jang et al., 2017](#)). Furthermore, avoiding optimization of covariance hyper-parameters bypasses the issue of bias in the optimization of hyper-parameters when combined with approximate inference techniques ([Li & Turner, 2016](#)).

For sparse GPs, [Hensman et al. \(2015b\)](#) argue that a Bayesian treatment of inducing inputs is unnecessary and arrive to the conclusion that the optimal prior $p(\mathbf{z})$ can be obtained by setting $p(\mathbf{Z}) = \delta(\mathbf{Z} - \hat{\mathbf{Z}})$, where $\hat{\mathbf{Z}}$ is the collection of inducing locations that minimizes the model fit term of the ELBO. We believe that, although mathematically correct, such a justification contradicts the fundamental principles of Bayesian inference as it relies on a ‘free-form’ optimization of the prior. If applied to any other model using variational inference, it would reduce the objective function to the model-fitting term in the ELBO, which indeed defeats the purpose of a Bayesian treatment. For a related discussion on this issue concerning Bayesian deep neural networks see [Graves \(2011\)](#).

3.1. Bayesian treatment of sparse Gaussian processes

Given that the inducing inputs do have an imprint on the modeling capabilities of sparse GPs, it is natural to consider them as model parameters and attempt to infer these along with inducing variables and covariance hyper-parameters. For this purpose, we propose Bayesian Sparse Gaussian Process (BSGP)—a fully-Bayesian treatment of sparse Gaussian process. The corresponding generative model, illustrated in [Figure 2c](#), is given as

$$\begin{aligned}
 \boldsymbol{\theta} &\sim p_{\boldsymbol{\theta}}(\boldsymbol{\theta}), \\
 \mathbf{Z} &\sim p_{\boldsymbol{\xi}}(\mathbf{Z}), \\
 \mathbf{u}|\mathbf{Z}, \boldsymbol{\theta} &\sim \mathcal{N}(\mathbf{0}, \mathbf{K}_{\mathbf{zz}|\boldsymbol{\theta}}), \\
 \mathbf{f}|\mathbf{u}, \mathbf{Z}, \boldsymbol{\theta} &\sim \mathcal{N}(\mathbf{K}_{\mathbf{xz}|\boldsymbol{\theta}}\mathbf{K}_{\mathbf{zz}|\boldsymbol{\theta}}^{-1}\mathbf{u}, \mathbf{K}_{\mathbf{xx}|\boldsymbol{\theta}, \mathbf{Z}}), \\
 \mathbf{y}|\mathbf{f}, \sigma^2 &\sim \mathcal{N}(\mathbf{f}, \sigma^2\mathbf{I}),
 \end{aligned} \tag{5}$$

where $\mathbf{K}_{\mathbf{x}\mathbf{x}|\boldsymbol{\theta}, \mathbf{Z}}$ denotes the covariance matrix obtained by conditioning in the joint model, i.e. $\mathbf{K}_{\mathbf{x}\mathbf{x}|\boldsymbol{\theta}, \mathbf{Z}} \equiv \mathbf{K}_{\mathbf{x}\mathbf{x}|\boldsymbol{\theta}} - \mathbf{K}_{\mathbf{x}\mathbf{z}|\boldsymbol{\theta}} \mathbf{K}_{\mathbf{z}\mathbf{z}|\boldsymbol{\theta}}^{-1} \mathbf{K}_{\mathbf{z}\mathbf{x}|\boldsymbol{\theta}}$. Although for simplicity we have specified a Gaussian conditional likelihood above, our approach does, in fact, handle other factorized conditional likelihood models. Figure 3 gives a pictorial illustration of the distribution over the covariance function induced by the posterior over inducing inputs computed at \mathbf{x}' for an RBF covariance function $k(\mathbf{x}, \mathbf{x}') = \sigma \exp(-\|\mathbf{x} - \mathbf{x}'\|^2 \lambda^{-2})$.

Given the model above, and following a similar analysis as that described in Section 2.1, we can obtain the optimal variational form that minimizes $\text{KL}[q(\mathbf{f}^*, \mathbf{f}, \mathbf{u}, \boldsymbol{\theta}) \parallel p(\mathbf{f}^*, \mathbf{f}, \mathbf{u}, \boldsymbol{\theta}|\mathbf{y})]$, where \mathbf{f}^* denotes functional values on all points of interest, a term well-defined even on infinite index sets (Matthews et al., 2016),

$$\log \hat{q}(\mathbf{u}, \mathbf{Z}, \boldsymbol{\theta}) = \mathbb{E}_{p(\mathbf{f}|\mathbf{u}, \mathbf{Z}, \boldsymbol{\theta})} \log p(\mathbf{y}|\mathbf{f}) + \log p(\mathbf{u}|\boldsymbol{\theta}, \mathbf{Z}) + \log p_{\boldsymbol{\xi}}(\mathbf{Z}) + \log p_{\psi}(\boldsymbol{\theta}) + \log C. \quad (6)$$

The intractability of an optimal q underlines the necessity of using MCMC to obtain samples from $\hat{q}(\mathbf{u}, \mathbf{Z}, \boldsymbol{\theta})$.

We can extend this formulation to deep GPs by compos-

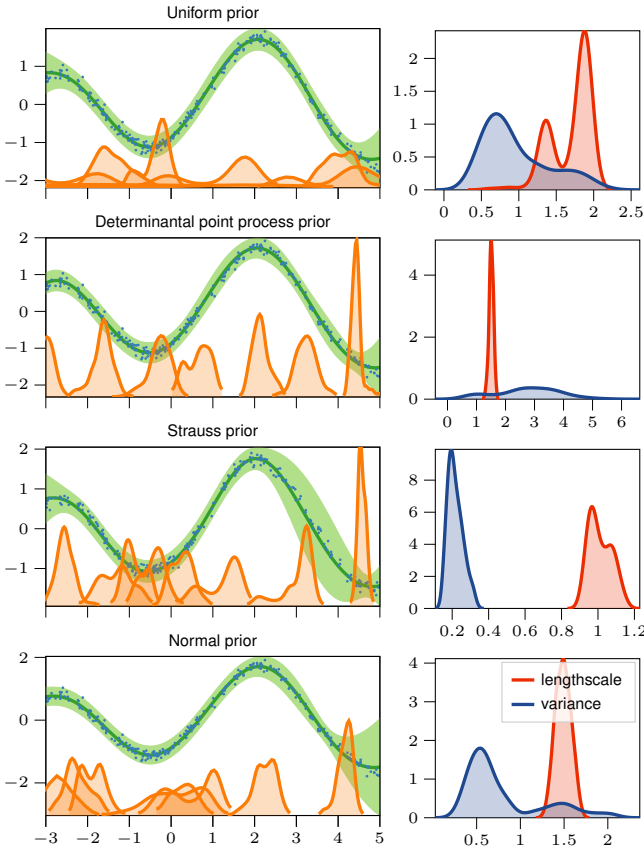


Figure 4: Comparison of the posterior over the inducing position $p(\mathbf{Z}|\mathbf{y})$ for different choices of prior. On the right, the posterior over covariance hyper-parameters $p(\lambda|\mathbf{y})$ and $p(\sigma|\mathbf{y})$.

ing sparse GPs. Assuming the likelihood $p(\mathbf{y}|\mathbf{f})$ factorizes over data points, and defining the energy function of the MCMC sampler over the joint space of inducing variables, inducing inputs and covariance hyper-parameters, $U(\mathbf{u}, \mathbf{Z}, \boldsymbol{\theta}) = -\log \hat{q}(\mathbf{u}, \mathbf{Z}, \boldsymbol{\theta}) + \log C$, we can obtain an unbiased estimate of U via Monte Carlo sampling (Salimbeni & Deisenroth, 2017) and a subsample of data,

$$\begin{aligned} U(\mathbf{u}, \mathbf{Z}, \boldsymbol{\theta}) &\approx -N \log p(y_i|\mathbf{f}_i) - \log p(\mathbf{u}|\boldsymbol{\theta}, \mathbf{Z}) \\ &\quad - \log p_{\boldsymbol{\xi}}(\mathbf{Z}) - \log p_{\psi}(\boldsymbol{\theta}), \\ \mathbf{f}_i &\sim p(\mathbf{f}_i|\mathbf{u}, \mathbf{Z}, \boldsymbol{\theta}, \mathbf{x}_i). \end{aligned}$$

We therefore obtain stochastic gradient estimates of U using the above approximation, and employ SGHMC.

3.2. Prior Choices

The prior $p(\mathbf{z}_1, \dots, \mathbf{z}_M)$ encodes our beliefs of the inducing location configuration, and it has a large effect on the resulting posteriors. The inducing locations support the resulting Gaussian process interpolation, which motivates matching the inducing prior to the data distribution $p(\mathbf{X})$. We begin by proposing a simple Normal (N) prior

$$p_N(\mathbf{Z}) = \prod_{j=1}^M \mathcal{N}(\mathbf{z}_j|\mathbf{0}, \mathbf{I}), \quad (7)$$

which matches the mean and variance of the normalized data distribution, and favors inducing locations toward the baricenter of the data inputs.

We also explore two more priors based on point processes, which consider distributions over point sets (González et al., 2016). Point processes can model repulsive effects to penalise clumped inducing points. The determinantal point process (DPP), defined as follows

$$p_D(\mathbf{Z}) \propto \det \mathbf{K}_{\mathbf{z}\mathbf{z}|\boldsymbol{\theta}}, \quad (8)$$

relates the probability of inducing locations to the volume of space spanned by the covariance (Lavancier et al., 2015). DPP is a repulsive point process, which gives higher probabilities to location diversity, controlled by the hyper-parameters $\boldsymbol{\xi} \equiv \boldsymbol{\theta}$. Alternatively we also consider the Strauss process (see e.g. Daley & Vere-Jones, 2003; Strauss, 1975),

$$p_S(\mathbf{Z}) \propto \lambda^M \gamma^{\sum_{\mathbf{z}, \mathbf{z}' \in \mathbf{Z}} \delta(|\mathbf{z} - \mathbf{z}'| < r)}, \quad (9)$$

where $\lambda > 0$ is the intensity, and $0 < \gamma \leq 1$ is the repulsion coefficient which decays the prior as a function of the number of location pairs that are within distance r . The Strauss prior (S) tends to maintain the minimum distance between inducing locations, parameterised by $\boldsymbol{\xi} = (\lambda, \gamma, r)$. We finally include a vanishing uninformative uniform prior (U), $\log p_U(\mathbf{Z}) = 0$, as a naive baseline for reference.

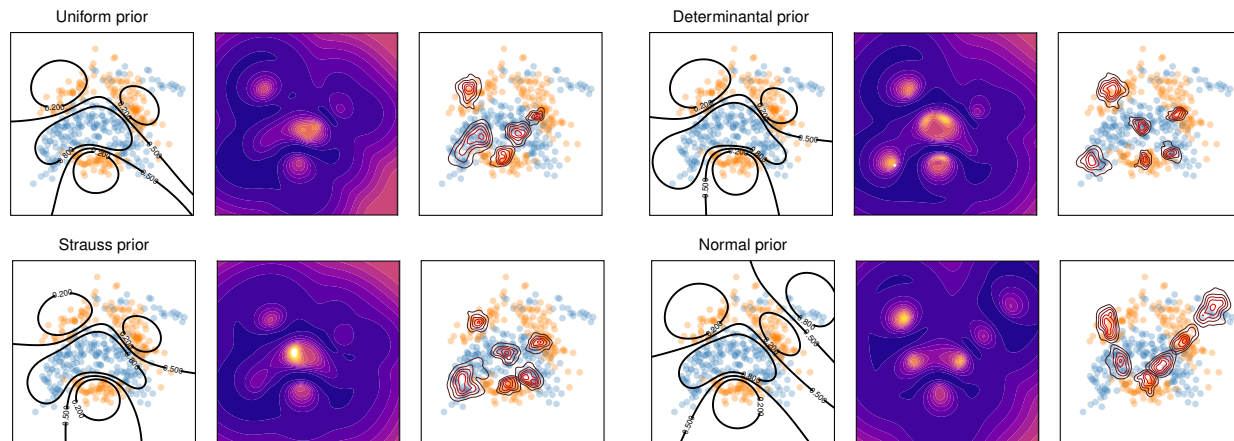


Figure 5: Illustrative example of a classification task on the BANANA dataset. On the left, the decision bounds of the average classifier. On the center, the entropy of the predictive distribution on the class labels, by means of fitting a Beta distribution, as a proxy to uncertainty quantification (the darker, the higher the entropy). On the right, the posterior marginals of the inducing inputs.

To gain insights on the choice of these priors, we set up a comparative analysis on a toy 1D regression task and on the BANANA dataset. Figure 4 visualizes the inducing location and kernel parameter posteriors with respect to the four priors on a 1D simulated toy dataset. We observe that the posterior densities on the inducing position are multimodal and highly non-Gaussian, further confirming the necessity of free form inference. Both Strauss and DPP priors lead approximately to evenly spread inducing locations. Figure 5 shows the inducing posteriors on a two-dimensional banana classification example, where accurate decision boundaries require some inducing location proximity, which results in the superior performance obtained by the Normal prior (N).

Prior on covariance hyper-parameters. Choosing a proper prior on the hyper-parameters has been discussed in previous works on Bayesian inference for GPs (see e.g. Filippone & Girolami, 2014). Throughout the paper, we use the RBF covariance with marginal variance σ and one lengthscale λ_i per feature (automatic relevance determination (Mackay, 1994)). On these two hyper-parameters we place a lognormal prior with unit variance and means equal to 1 and 0.05 for λ and σ , respectively.

4. Experiments

In this section, we will provide empirical evidence of the benefits of BSGP in shallow and deep GPs.

4.1. UCI benchmark

We start our evaluation with a benchmark on 8 small to moderate sized UCI regression datasets. The input points and targets are normalized with zero mean and unit variance. We perform 8 different splits of train/test set with 0.8/0.2 ra-

tio, and train the different models for 10,000 iterations with a learning rate fixed at 0.01 and a minibatch size of 1,000 samples. We then proceed to collect 256 samples, used for computing the predictive test metrics. We compare against two current state-of-the-art deep GP methods SGHMC-DGP (Havasi et al., 2018b) and IPVI-DGP (Yu et al., 2019), and against the shallow SVGP baseline (Hensman et al., 2015a). For a faithful comparison with IPVI-DGP we follow their recommended parameter configurations¹. All models share $M = 100$ inducing points, the same RBF covariance with automatic relevance determination (ARD) and, for DGP, the same hidden dimensions (equal to the input dimension D). BSGP has a normal prior on the inducing locations $p(\mathbf{Z})$ and lognormal prior on the lengthscales $p(\lambda)$ and the variance $p(\sigma)$ of the covariance function.

Figure 6 shows the predictive test MNLL mean and 95% CI over the different folds over the UCI datasets, and also includes rank summaries. The proposed method clearly outperforms competing deep and shallow GPs. The improvements are particularly evident on NAVAL, a dataset known to be easy to fit and therefore challenging to improve upon. Furthermore, the deeper models perform consistently better or on par with the shallow version, without incurring in any measurable overfitting even on small or medium datasets (See BOSTON and YACHT, for example).

Choosing the prior. As described in Section 3.2, we propose different types of priors on the inducing positions: determinantal point process prior, standard normal prior, Strauss prior and uniform. Next, we compare the performance of the four priors on a single layer BSGP over the UCI datasets (see Figure 7). The results show that the

¹We use the IPVI-DGP implementation available at github.com/HeroKillerEver/ipvi-dgp

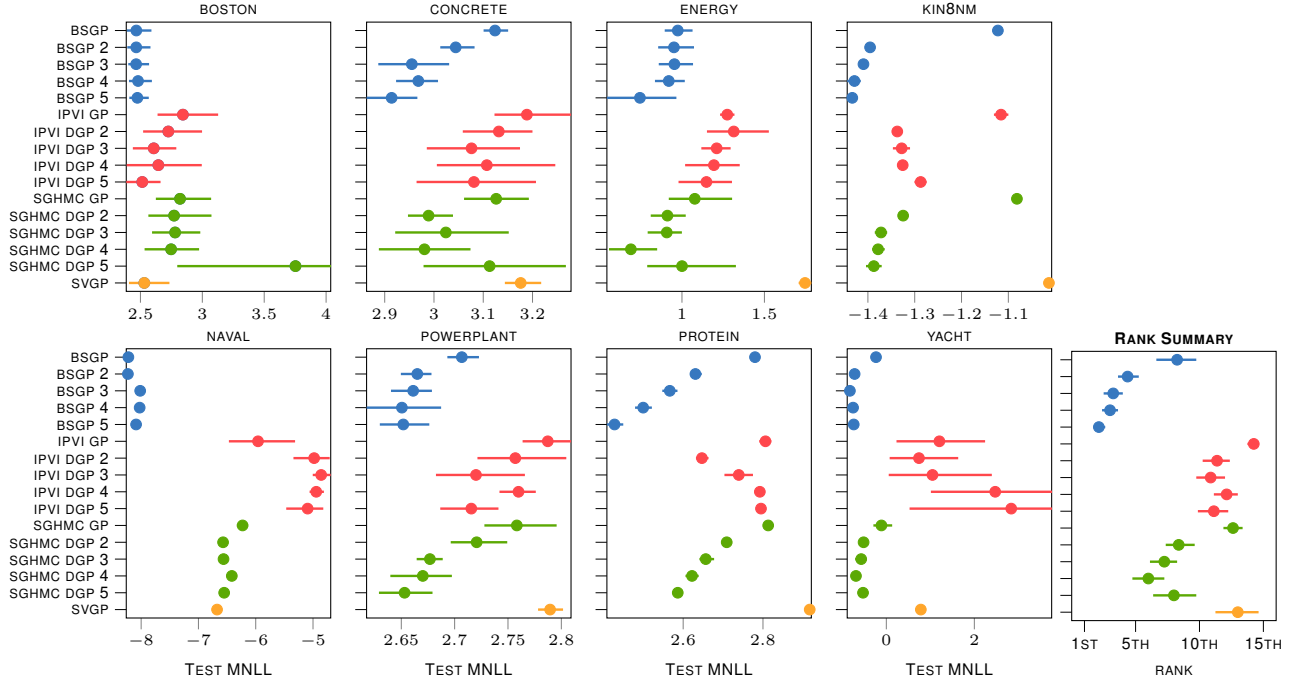


Figure 6: Test MNLL on UCI regression benchmark (the error bars represent the 95%CI). The lower MNLL (i.e. to the left), the better. The number on the right of the method’s name refers to the depth of the DGP.

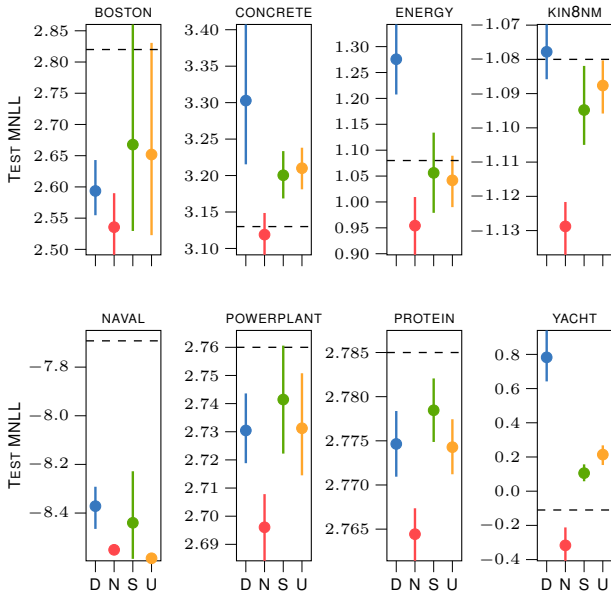


Figure 7: Comparison with different prior, on a single layer GP with 100 inducing variables (mean and 95%CI showed). The labels corresponds to D for determinantal, N for normal, S for Strauss and U for uniform. The dashed-line corresponds to the baseline of SGHMC.

Normal prior consistently outperforms other priors. The uniform and Strauss priors behave similarly, while the De-

terminantal prior has the largest variance.

A comment on computational efficiency. Similarly to the competing baseline algorithms, each iteration of BSGP involves the computation of the covariance matrix and its inverse with complexity $\mathcal{O}(M^3)$. Computing the predictive distribution, on the other hand, is more challenging as it requires recomputing the covariance matrices \mathbf{K}_{xz} , \mathbf{K}_{zz} for each posterior sample \mathbf{Z} , for an overall complexity linear on the number of posterior samples. Nonetheless, this operation can be parallelized, thus taking full advantage of the high-performance parallel computing power of GPUs.

We show this trade-off in practice for a shallow GP and a 2-layer DGP in Figure 8, where we compare the three main methods with a fixed training time budget of one hour. The experiment is repeated four times on the same fold and

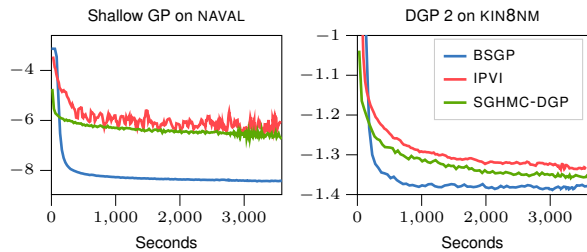


Figure 8: Comparison of test MNLL as function of training time.

Table 2: Average number of gradient evaluations per second on CPU. Minibatch size fixed to 1,000 examples.

	GP (NAVAL)	DGP-2 (KIN8NM)
BSGP	38.0	21.4
IPVI	21.5	9.3
SGHMC	60.3	31.3

the results are then averaged. Each run is performed on an isolated instance in a cloud computing platform with 8 CPU cores and 8 GB of memory reserved. Inference on the test set is performed every 250 iterations.

BSGP converges dramatically faster in wall-clock time into superior solutions over state-of-the-art competing methods (although the single gradient step requires a bit more time – see Table 2).

4.2. Large scale classification

The AIRLINE dataset is a classic benchmark for large scale prediction task. It collects all commercial flights in USA during 2008, counting more than 5 millions data points. The goal is to find if a flight will be delayed based on 8 features, namely *month*, *day of month*, *day of week*, *airtime*, *distance*, *arrival time*, *departure time* and *age* of the plane. We preprocess the dataset following the guidelines provided by Hensman et al. (2015b) and Wilson et al. (2016a).

After a burn-in phase of 10,000 iterations, we draw 200 samples with 1000 simulation steps in between. We test on 100,000 randomly selected held-out points. We fit three models with $M = 100$ inducing points. Table 3 shows the predictive performance of three shallow GP models over test fold. The BSGP improves upon both inference methods of SGHMC-GP and SVGP over all criteria of test error, test MNLL and test area under the curve (AUC). We assess the convergence of the predictive posterior by evaluating the \hat{R} -statistics (Gelman et al., 2004) over 4 SGHMC sampler chains. The \hat{R} compares the within-chain vari-

Table 3: AIRLINE dataset predictive test performance.

Model	error (\downarrow)	MNLL (\downarrow)	AUC (\uparrow)
SGHMC-GP	35.85%	0.646	0.671
SVGP	31.26%	0.595	0.730
BSGP	30.46%	0.580	0.749

Table 4: HIGGS dataset predictive test performance.

Model	error (\downarrow)	MNLL (\downarrow)	AUC (\uparrow)
SGHMC-GP	35.39%	0.628	0.698
SVGP	27.79%	0.544	0.796
BSGP	26.97%	0.530	0.808

ance to between-chain variance. This diagnostic yielded a $\hat{R} = 1.02 \pm 0.045$, which indicates good convergence. Finally, we visualise the prediction marginals and the trace for 3 test points for further indication of mixing in the Supplements.

As a final large scale test, we opt for the HIGGS dataset (Baldi et al., 2014). With 11 millions data points and 28 features each, this dataset was created by Monte Carlo simulations of particle dynamics in accelerators to help detecting the Higgs boson. We select 90% of the these points for training, while the rest is kept for testing. Table 4 reports the final test performance, showing that BSGP outperforms the competitive methods. Interestingly, in both these large scale experiments, SGHMC-GP always falls back considerably w.r.t. BSGP and even SVGP. We argue that, with these large sized datasets, the continuous alternation of optimization of \mathbf{Z} and θ and sampling of \mathbf{U} used by the Authors (called Moving Window MCEM – see Havasi et al. (2018a) for further details) might have lead to suboptimal solutions.

5. Conclusion & Discussion

We have developed a fully Bayesian treatment of sparse Gaussian process models that considers the inducing inputs, along with the inducing variables and covariance hyper-parameters, as random variables, places suitable priors and carries out approximate inference over them. Our approach, based on SGHMC, investigated two conventional priors (Gaussian and uniform) for the inducing inputs as well as two point process based priors (the Determinantal and the Strauss processes).

By challenging the standard belief of most previous work on sparse GP inference that assumes the inducing inputs can be estimated point-wisely, we have developed a state-of-the-art inference method and have demonstrated its outstanding performance on both accuracy and running time on regression and classification problems. We hope this work can have an impact similar (or better) to other works in machine learning that have adopted more elaborate Bayesian machinery (e.g. Wallach et al., 2009) for long-standing inference problems in commonly used probabilistic models.

Finally, we believe it is worth investigating further more structured priors similar to those presented here (e.g. exploring different hyper-parameter settings), including a full joint treatment of inducing inputs and their number, i.e. $p(\mathbf{Z}, M)$. We leave this as future work. We are currently investigating ways to extend BSGP to convolutional Gaussian process (van der Wilk et al., 2017; Dutordoir et al., 2019; Blomqvist et al., 2018).

Acknowledgements MF gratefully acknowledges support from the AXA Research Fund.

References

- Baldi, P., Sadowski, P., and Whiteson, D. Searching for exotic particles in high-energy physics with deep learning. *Nature Communications*, 5(1):4308, 2014.
- Barber, D. and Williams, C. K. Gaussian processes for Bayesian classification via hybrid Monte Carlo. In *Advances in neural information processing systems*, pp. 340–346, 1997.
- Blomqvist, K., Kaski, S., and Heinonen, M. Deep convolutional gaussian processes. *CoRR*, abs/1810.03052, 2018.
- Bonilla, E. V., Krauth, K., and Dezfouli, A. Generic inference in latent Gaussian process models. *Journal of Machine Learning Research*, 20(117):1–63, 2019.
- Chen, T., Fox, E., and Guestrin, C. Stochastic Gradient Hamiltonian Monte Carlo. In Xing, E. P. and Jebara, T. (eds.), *Proceedings of the 31st International Conference on Machine Learning*, volume 32 of *Proceedings of Machine Learning Research*, pp. 1683–1691, Beijing, China, 22–24 Jun 2014. PMLR.
- Cutajar, K., Bonilla, E. V., Michiardi, P., and Filippone, M. Random feature expansions for deep Gaussian processes. In Precup, D. and Teh, Y. W. (eds.), *Proceedings of the 34th International Conference on Machine Learning*, volume 70 of *Proceedings of Machine Learning Research*, pp. 884–893, International Convention Centre, Sydney, Australia, August 2017. PMLR.
- Daley, D. J. and Vere-Jones, D. *An introduction to the theory of point processes. Vol. I. Probability and its Applications* (New York). Springer-Verlag, second edition, 2003. Elementary theory and methods.
- Damianou, A. C. and Lawrence, N. D. Deep Gaussian Processes. In *Proceedings of the Sixteenth International Conference on Artificial Intelligence and Statistics, AISTATS 2013, Scottsdale, AZ, USA, April 29 - May 1, 2013*, volume 31 of *JMLR Proceedings*, pp. 207–215. JMLR.org, 2013.
- Duane, S., Kennedy, A., Pendleton, B. J., and Roweth, D. Hybrid Monte Carlo. *Physics Letters B*, 195(2):216 – 222, 1987.
- Dutordoir, V., van der Wilk, M., Artemev, A., Tomczak, M., and Hensman, J. Translation Insensitivity for Deep Convolutional Gaussian Processes. *arXiv e-prints*, art. arXiv:1902.05888, Feb 2019.
- Filippone, M. and Girolami, M. Pseudo-marginal Bayesian inference for Gaussian processes. *IEEE Transactions on Pattern Analysis and Machine Intelligence*, 36(11): 2214–2226, 2014.
- Gal, Y. and Ghahramani, Z. Dropout As a Bayesian Approximation: Representing Model Uncertainty in Deep Learning. In *Proceedings of the 33rd International Conference on International Conference on Machine Learning - Volume 48, ICML’16*, pp. 1050–1059. JMLR.org, 2016.
- Gelman, A., Carlin, J. B., Stern, H. S., and Rubin, D. B. *Bayesian Data Analysis*. Chapman and Hall/CRC, 2nd ed. edition, 2004.
- González, J. A., Rodríguez-Cortés, F. J., Cronie, O., and Mateu, J. Spatio-temporal point process statistics: a review. *Spatial Statistics*, 18:505–544, 2016.
- Graves, A. Practical Variational Inference for Neural Networks. In Shawe-Taylor, J., Zemel, R. S., Bartlett, P. L., Pereira, F., and Weinberger, K. Q. (eds.), *Advances in Neural Information Processing Systems 24*, pp. 2348–2356. Curran Associates, Inc., 2011.
- Havasi, M., Hernández-Lobato, J. M., and Murillo-Fuentes, J. J. Inference in Deep Gaussian Processes using Stochastic Gradient Hamiltonian Monte Carlo, June 2018a. arXiv:1806.05490.
- Havasi, M., Hernández-Lobato, J. M., and Murillo-Fuentes, J. J. Inference in Deep Gaussian Processes using Stochastic Gradient Hamiltonian Monte Carlo. In Bengio, S., Wallach, H., Larochelle, H., Grauman, K., Cesa-Bianchi, N., and Garnett, R. (eds.), *Advances in Neural Information Processing Systems 31*, pp. 7506–7516. Curran Associates, Inc., 2018b.
- Hensman, J., Fusi, N., and Lawrence, N. D. Gaussian processes for big data. In *Proceedings of the Twenty-Ninth Conference on Uncertainty in Artificial Intelligence, UAI13*, pp. 282290, Arlington, Virginia, USA, 2013. AUAI Press.
- Hensman, J., Matthews, A., and Ghahramani, Z. Scalable Variational Gaussian Process Classification. In Lebanon, G. and Vishwanathan, S. V. N. (eds.), *Proceedings of the Eighteenth International Conference on Artificial Intelligence and Statistics*, volume 38 of *Proceedings of Machine Learning Research*, pp. 351–360, San Diego, California, USA, May 2015a. PMLR.
- Hensman, J., Matthews, A. G., Filippone, M., and Ghahramani, Z. MCMC for Variationally Sparse Gaussian Processes. In Cortes, C., Lawrence, N. D., Lee, D. D., Sugiyama, M., and Garnett, R. (eds.), *Advances in Neural Information Processing Systems 28*, pp. 1648–1656. Curran Associates, Inc., 2015b.
- Jang, P. A., Loeb, A., Davidow, M., and Wilson, A. G. Scalable Lévy process priors for spectral kernel learning.

- In *Advances in Neural Information Processing Systems*, pp. 3940–3949, 2017.
- Jordan, M. I., Ghahramani, Z., Jaakkola, T. S., and Saul, L. K. An Introduction to Variational Methods for Graphical Models. *Machine Learning*, 37(2):183–233, November 1999.
- Krauth, K., Bonilla, E. V., Cutajar, K., and Filippone, M. AutoGP: Exploring the capabilities and limitations of Gaussian process models. In *Thirty-Third Conference on Uncertainty in Artificial Intelligence, UAI 2017, August 11-15, 2017, Sydney, Australia*, 2017.
- Lavancier, F., Mller, J., and Rubak, E. Determinantal point process models and statistical inference. *Royal Statistical Society B*, 77:853–877, 2015.
- Lawrence, N. Probabilistic Non-linear Principal Component Analysis with Gaussian Process Latent Variable Models. *Journal of Machine Learning Research*, 6:1783–1816, December 2005.
- Lázaro-Gredilla, M. and Figueiras-Vidal, A. Inter-domain Gaussian Processes for Sparse Inference using Inducing Features. In Bengio, Y., Schuurmans, D., Lafferty, J. D., Williams, C. K. I., and Culotta, A. (eds.), *Advances in Neural Information Processing Systems 22*, pp. 1087–1095. Curran Associates, Inc., 2009.
- Lázaro-Gredilla, M., Quinero-Candela, J., Rasmussen, C. E., and Figueiras-Vidal, A. R. Sparse Spectrum Gaussian Process Regression. *Journal of Machine Learning Research*, 11:1865–1881, 2010.
- Li, Y. and Turner, R. E. Rényi divergence variational inference. In Lee, D. D., Sugiyama, M., Luxburg, U. V., Guyon, I., and Garnett, R. (eds.), *Advances in Neural Information Processing Systems 29*, pp. 1073–1081. Curran Associates, Inc., 2016.
- Mackay, D. J. C. Bayesian methods for backpropagation networks. In Domany, E., van Hemmen, J. L., and Schulten, K. (eds.), *Models of Neural Networks III*, chapter 6, pp. 211–254. Springer, 1994.
- Matthews, A. G., van der Wilk, M., Nickson, T., Fujii, K., Boukouvalas, A., León-Villagrà, P., Ghahramani, Z., and Hensman, J. GPflow: A Gaussian process library using TensorFlow. *Journal of Machine Learning Research*, 18(40):1–6, April 2017.
- Matthews, A. G. d. G., Hensman, J., Turner, R., and Ghahramani, Z. On sparse variational methods and the Kullback-Leibler divergence between stochastic processes. In *Artificial Intelligence and Statistics*, pp. 231–239, 2016.
- Murray, I. and Adams, R. P. Slice sampling covariance hyperparameters of latent Gaussian models. In Lafferty, J. D., Williams, C. K. I., Shawe-Taylor, J., Zemel, R. S., and Culotta, A. (eds.), *Advances in Neural Information Processing Systems 23: 24th Annual Conference on Neural Information Processing Systems 2010. Proceedings of a meeting held 6-9 December 2010, Vancouver, British Columbia, Canada.*, pp. 1732–1740. Curran Associates, Inc., 2010.
- Neal, R. M. Monte Carlo implementation of Gaussian process models for Bayesian regression and classification. *Technical Report*, 1997.
- Neal, R. M. MCMC using Hamiltonian dynamics. *Handbook of Markov Chain Monte Carlo*, 54:113–162, 2010.
- Rahimi, A. and Recht, B. Random Features for Large-Scale Kernel Machines. In Platt, J. C., Koller, D., Singer, Y., and Roweis, S. T. (eds.), *Advances in Neural Information Processing Systems 20*, pp. 1177–1184. Curran Associates, Inc., 2008.
- Rasmussen, C. E. and Williams, C. *Gaussian Processes for Machine Learning*. MIT Press, 2006.
- Rasmussen, C. E. and Williams, C. K. I. *Gaussian Processes for Machine Learning (Adaptive Computation and Machine Learning)*. The MIT Press, 2005.
- Saatçi, Y. *Scalable Inference for Structured Gaussian Process Models*. PhD thesis, University of Cambridge, 2011.
- Salimbeni, H. and Deisenroth, M. Doubly Stochastic Variational Inference for Deep Gaussian Processes. In Guyon, I., Luxburg, U. V., Bengio, S., Wallach, H., Fergus, R., Vishwanathan, S., and Garnett, R. (eds.), *Advances in Neural Information Processing Systems 30*, pp. 4588–4599. Curran Associates, Inc., 2017.
- Shi, J., Titsias, M. K., and Mnih, A. Sparse orthogonal variational inference for gaussian processes. *arXiv preprint arXiv:1910.10596*, 2019.
- Snelson, E. and Ghahramani, Z. Sparse Gaussian Processes using Pseudo-inputs. In *NIPS*, 2005.
- Springenberg, J. T., Klein, A., Falkner, S., and Hutter, F. Bayesian Optimization with Robust Bayesian Neural Networks. In Lee, D. D., Sugiyama, M., Luxburg, U. V., Guyon, I., and Garnett, R. (eds.), *Advances in Neural Information Processing Systems 29*, pp. 4134–4142. Curran Associates, Inc., 2016.
- Strauss, D. J. A model for clustering. *Biometrika*, 62(2): 467–475, 08 1975.

- Titsias, M. and Lawrence, N. D. Bayesian gaussian process latent variable model. In *Proceedings of the Thirteenth International Conference on Artificial Intelligence and Statistics*, pp. 844–851, 2010.
- Titsias, M. K. Variational Learning of Inducing Variables in Sparse Gaussian Processes. In Dyk, D. A. and Welling, M. (eds.), *Proceedings of the Twelfth International Conference on Artificial Intelligence and Statistics, AISTATS 2009, Clearwater Beach, Florida, USA, April 16-18, 2009*, volume 5 of *JMLR Proceedings*, pp. 567–574. JMLR.org, 2009.
- van der Wilk, M., Rasmussen, C. E., and Hensman, J. Convolutional Gaussian Processes. In Guyon, I., Luxburg, U. V., Bengio, S., Wallach, H., Fergus, R., Vishwanathan, S., and Garnett, R. (eds.), *Advances in Neural Information Processing Systems 30*, pp. 2849–2858. Curran Associates, Inc., 2017.
- Wallach, H. M., Mimno, D. M., and McCallum, A. Rethinking LDA: Why priors matter. In Bengio, Y., Schuurmans, D., Lafferty, J. D., Williams, C. K. I., and Culotta, A. (eds.), *Advances in Neural Information Processing Systems 22*, pp. 1973–1981. Curran Associates, Inc., 2009.
- Wilson, A. and Nickisch, H. Kernel Interpolation for Scalable Structured Gaussian Processes (KISS-GP). In Blei, D. and Bach, F. (eds.), *Proceedings of the 32nd International Conference on Machine Learning (ICML-15)*, pp. 1775–1784. JMLR Workshop and Conference Proceedings, 2015.
- Wilson, A. G., Hu, Z., Salakhutdinov, R., and Xing, E. P. Deep Kernel Learning. In Gretton, A. and Robert, C. C. (eds.), *Proceedings of the 19th International Conference on Artificial Intelligence and Statistics*, volume 51 of *Proceedings of Machine Learning Research*, pp. 370–378, Cadiz, Spain, May 2016a. PMLR.
- Wilson, A. G., Hu, Z., Salakhutdinov, R. R., and Xing, E. P. Stochastic Variational Deep Kernel Learning. In Lee, D. D., Sugiyama, M., Luxburg, U. V., Guyon, I., and Garnett, R. (eds.), *Advances in Neural Information Processing Systems 29*, pp. 2586–2594. Curran Associates, Inc., 2016b.
- Yu, H., Chen, Y., Low, B. K. H., Jaillet, P., and Dai, Z. Implicit Posterior Variational Inference for Deep Gaussian Processes. In Wallach, H., Larochelle, H., Beygelzimer, A., d’Alché Buc, F., Fox, E., and Garnett, R. (eds.), *Advances in Neural Information Processing Systems 32*, pp. 14475–14486. Curran Associates, Inc., 2019.

A. Derivation for Deep Gaussian Processes

In this section, we derive the the mathematical basis for of Bayesian treatment of inducing inputs in a DGP setting (Damianou & Lawrence, 2013). This derivation extends the one in Section 2 of Hensman et al. (2015b), where we add deep GPs, prior on inducing inputs and stochastic gradients. We assume a deep Gaussian process prior $f^L \circ f^{L-1} \circ \dots \circ f^1$, where each f^ℓ is a GP. For notational brevity, we use θ^ℓ as both kernel hyper-parameters and inducing inputs of the ℓ -th layer, and \mathbf{f}^0 as the input vector \mathbf{X} . We also denote \mathbf{f}_*^ℓ as the latent function values for layer ℓ at other input points of interest. Then we can write down the joint distribution over visible and latent variables (omitting the dependency on \mathbf{X} for clarity) as

$$p\left(\mathbf{y}, \left\{\mathbf{f}^\ell, \mathbf{u}^\ell, \boldsymbol{\theta}^\ell\right\}_{\ell=1}^L\right) = p\left(\mathbf{y} \mid \mathbf{f}^L\right) \prod_{\ell=1}^L p\left(\mathbf{f}^\ell \mid \mathbf{u}^\ell, \mathbf{f}^{\ell-1}, \boldsymbol{\theta}^\ell\right) p\left(\mathbf{u}^\ell \mid \boldsymbol{\theta}^\ell\right) p\left(\boldsymbol{\theta}^\ell\right). \quad (10)$$

Our goal is to estimate the posterior $p\left(\left\{\mathbf{f}^\ell, \mathbf{u}^\ell, \boldsymbol{\theta}^\ell\right\}_{\ell=1}^L \mid \mathbf{y}\right)$, which we can use to compute the predictive distribution

$$p\left(\mathbf{f}_*^L \mid \mathbf{y}\right) = \int p\left(\left\{\mathbf{f}_*^\ell\right\}_{\ell=1}^L \mid \left\{\mathbf{f}^\ell, \mathbf{u}^\ell, \boldsymbol{\theta}^\ell\right\}_{\ell=1}^L\right) p\left(\left\{\mathbf{f}^\ell, \mathbf{u}^\ell, \boldsymbol{\theta}^\ell\right\}_{\ell=1}^L \mid \mathbf{y}\right) d\left\{\mathbf{f}_*^\ell\right\}_{\ell=1}^{L-1}, \left\{\mathbf{f}^\ell, \mathbf{u}^\ell, \boldsymbol{\theta}^\ell\right\}_{\ell=1}^L. \quad (11)$$

Given that the posterior $p\left(\left\{\mathbf{f}^\ell, \mathbf{u}^\ell, \boldsymbol{\theta}^\ell\right\}_{\ell=1}^L \mid \mathbf{y}\right)$ is intractable, we can use the following variational approximation over all latent variables (including $\{\mathbf{f}_*^\ell\}$):

$$q\left(\left\{\mathbf{f}_*^\ell, \mathbf{f}^\ell, \mathbf{u}^\ell, \boldsymbol{\theta}^\ell\right\}_{\ell=1}^L\right) = p\left(\left\{\mathbf{f}_*^\ell\right\}_{\ell=1}^L \mid \left\{\mathbf{f}^\ell, \mathbf{u}^\ell, \boldsymbol{\theta}^\ell\right\}_{\ell=1}^L\right) \prod_{\ell=1}^L p\left(\mathbf{f}^\ell \mid \mathbf{u}^\ell, \mathbf{f}^{\ell-1}, \boldsymbol{\theta}^\ell\right) q\left(\left\{\mathbf{u}^\ell, \boldsymbol{\theta}^\ell\right\}_{\ell=1}^L\right). \quad (12)$$

where, analogously to the GP case, we have used the exact conditionals $p(\{\mathbf{f}_*^\ell\}_{\ell=1}^L \mid \{\mathbf{f}^\ell, \mathbf{u}^\ell, \boldsymbol{\theta}^\ell\}_{\ell=1}^L)$ and $\{p(\mathbf{f}^\ell \mid \mathbf{u}^\ell, \mathbf{f}^{\ell-1}, \boldsymbol{\theta}^\ell)\}$. More importantly, we will let the variational posterior over inducing variables and hyper-parameters (including inducing inputs) $q(\{\mathbf{u}^\ell, \boldsymbol{\theta}^\ell\}_{\ell=1}^L)$ be a free-form distribution which we will sample from. In order to obtain this optimal posterior, we can thus minimize the KL-divergence between the approximate posterior $q(\{\mathbf{f}_*^\ell, \mathbf{f}^\ell, \mathbf{u}^\ell, \boldsymbol{\theta}^\ell\}_{\ell=1}^L)$ and the true posterior $p(\{\mathbf{f}_*^\ell, \mathbf{f}^\ell, \mathbf{u}^\ell, \boldsymbol{\theta}^\ell\}_{\ell=1}^L \mid \mathbf{y})$ as follows,

$$\begin{aligned} & \text{KL}\left[q\left(\left\{\mathbf{f}_*^\ell, \mathbf{f}^\ell, \mathbf{u}^\ell, \boldsymbol{\theta}^\ell\right\}_{\ell=1}^L\right) \parallel p\left(\left\{\mathbf{f}_*^\ell, \mathbf{f}^\ell, \mathbf{u}^\ell, \boldsymbol{\theta}^\ell\right\}_{\ell=1}^L \mid \mathbf{y}\right)\right] \\ &= -\mathbb{E}_{q(\{\mathbf{f}_*^\ell, \mathbf{f}^\ell, \mathbf{u}^\ell, \boldsymbol{\theta}^\ell\}_{\ell=1}^L)} \left[\log \frac{p\left(\left\{\mathbf{f}_*^\ell\right\}_{\ell=1}^L \mid \left\{\mathbf{f}^\ell, \mathbf{u}^\ell, \boldsymbol{\theta}^\ell\right\}_{\ell=1}^L\right) p\left(\left\{\mathbf{f}^\ell, \mathbf{u}^\ell, \boldsymbol{\theta}^\ell\right\}_{\ell=1}^L \mid \mathbf{y}\right)}{p\left(\left\{\mathbf{f}_*^\ell\right\}_{\ell=1}^L \mid \left\{\mathbf{f}^\ell, \mathbf{u}^\ell, \boldsymbol{\theta}^\ell\right\}_{\ell=1}^L\right) q\left(\left\{\mathbf{f}^\ell, \mathbf{u}^\ell, \boldsymbol{\theta}^\ell\right\}_{\ell=1}^L\right)} \right] \\ &= -\mathbb{E}_{q(\{\mathbf{f}^\ell, \mathbf{u}^\ell, \boldsymbol{\theta}^\ell\}_{\ell=1}^L)} \left[\log \frac{p\left(\mathbf{y} \mid \mathbf{f}^L\right) \prod_{\ell=1}^L p\left(\mathbf{f}^\ell \mid \mathbf{u}^\ell, \mathbf{f}^{\ell-1}, \boldsymbol{\theta}^\ell\right) \prod_{\ell=1}^L p\left(\mathbf{u}^\ell \mid \boldsymbol{\theta}^\ell\right) p\left(\boldsymbol{\theta}^\ell\right) / p(\mathbf{y})}{\prod_{\ell=1}^L p\left(\mathbf{f}^\ell \mid \mathbf{u}^\ell, \mathbf{f}^{\ell-1}, \boldsymbol{\theta}^\ell\right) q\left(\left\{\mathbf{u}^\ell, \boldsymbol{\theta}^\ell\right\}_{\ell=1}^L\right)} \right] \\ &= -\mathbb{E}_{p(\{\mathbf{f}^\ell\} \mid \{\mathbf{u}^\ell, \boldsymbol{\theta}^\ell\}) q(\{\mathbf{u}^\ell, \boldsymbol{\theta}^\ell\}_{\ell=1}^L)} \left[\log \frac{p\left(\mathbf{y} \mid \mathbf{f}^L\right) \prod_{\ell=1}^L p\left(\mathbf{u}^\ell \mid \boldsymbol{\theta}^\ell\right) p\left(\boldsymbol{\theta}^\ell\right)}{q\left(\left\{\mathbf{u}^\ell, \boldsymbol{\theta}^\ell\right\}_{\ell=1}^L\right)} \right] + \log p(\mathbf{y}) \\ &= -\mathbb{E}_{q(\{\mathbf{u}^\ell, \boldsymbol{\theta}^\ell\}_{\ell=1}^L)} \left[\log \frac{e^{\mathbb{E}_{p(\{\mathbf{f}^\ell\} \mid \{\mathbf{u}^\ell, \boldsymbol{\theta}^\ell\}) \log p(\mathbf{y} \mid \mathbf{f}^L)}} \prod_{\ell=1}^L p\left(\mathbf{u}^\ell \mid \boldsymbol{\theta}^\ell\right) p\left(\boldsymbol{\theta}^\ell\right)}{q\left(\left\{\mathbf{u}^\ell, \boldsymbol{\theta}^\ell\right\}_{\ell=1}^L\right)} \right] + \log p(\mathbf{y}) \\ &= -\mathbb{E}_{q(\{\mathbf{u}^\ell, \boldsymbol{\theta}^\ell\}_{\ell=1}^L)} \left[\log \frac{e^{\mathbb{E}_{p(\{\mathbf{f}^\ell\} \mid \{\mathbf{u}^\ell, \boldsymbol{\theta}^\ell\}) \log p(\mathbf{y} \mid \mathbf{f}^L)}} \prod_{\ell=1}^L p\left(\mathbf{u}^\ell \mid \boldsymbol{\theta}^\ell\right) p\left(\boldsymbol{\theta}^\ell\right) / C}{q\left(\left\{\mathbf{u}^\ell, \boldsymbol{\theta}^\ell\right\}_{\ell=1}^L\right)} \right] - \log C + \log p(\mathbf{y}) \end{aligned}$$

$$= \text{KL} \left[q \left(\left\{ \mathbf{u}^\ell, \boldsymbol{\theta}^\ell \right\}_{\ell=1}^L \right) \parallel e^{\mathbb{E}_p(\{\mathbf{f}^\ell\}|\{\mathbf{u}^\ell, \boldsymbol{\theta}^\ell\}) \log p(\mathbf{y}|\mathbf{f}^L)} \prod_{\ell=1}^L p(\mathbf{u}^\ell | \boldsymbol{\theta}^\ell) p(\boldsymbol{\theta}^\ell) / C \right] - \log C + \log p(\mathbf{y}) \quad (13)$$

$$\geq -\log C + \log p(\mathbf{y}). \quad (14)$$

Here C is a normalizing constant $C = \int e^{\mathbb{E}_p(\{\mathbf{f}^\ell\}|\{\mathbf{u}^\ell, \boldsymbol{\theta}^\ell\}) \log p(\mathbf{y}|\mathbf{f}^L)} \prod_{\ell=1}^L p(\mathbf{u}^\ell | \boldsymbol{\theta}^\ell) p(\boldsymbol{\theta}^\ell) d\{\mathbf{u}^\ell, \boldsymbol{\theta}^\ell\}_{\ell=1}^L$, and the KL-divergence term is minimized when the KL term in Equation 13 equals 0, i.e.,

$$\log \hat{q} \left(\left\{ \mathbf{u}^\ell, \boldsymbol{\theta}^\ell \right\}_{\ell=1}^L \right) = \mathbb{E}_p(\{\mathbf{f}^\ell\}|\{\mathbf{u}^\ell, \boldsymbol{\theta}^\ell\}) \left[\log p(\mathbf{y} | \mathbf{f}^L) \right] + \sum_{\ell=1}^L \left(\log p(\mathbf{u}^\ell | \boldsymbol{\theta}^\ell) + \log p(\boldsymbol{\theta}^\ell) \right) - \log C. \quad (15)$$

While the optimal distribution \hat{q} is intractable, we have obtained the form of its (un-normalized) log joint, from which we can sample using HMC methods. However, Equation 15 is not immediately computable owing to the intractable expectation term. More calculations reveal that we can, nevertheless, obtain unbiased estimates of this expectation term with Monte Carlo sampling and data subsampling (Salimbeni & Deisenroth, 2017), assuming that the conditional likelihood $p(\mathbf{y}|\mathbf{f}^L)$ factorizes over datapoints,

$$\begin{aligned} \mathbb{E}_p(\{\mathbf{f}^\ell\}|\{\mathbf{u}^\ell, \boldsymbol{\theta}^\ell\}) \left[\log p(\mathbf{y} | \mathbf{f}^L) \right] &\approx \mathbb{E}_p(\{\mathbf{f}^\ell\}_{\ell=2}^L | \tilde{\mathbf{f}}^1, \{\mathbf{u}^\ell, \boldsymbol{\theta}^\ell\}_{\ell=2}^L) \left[\log p(\mathbf{y} | \mathbf{f}^L) \right], \tilde{\mathbf{f}}^1 \sim p(\mathbf{f}^1 | \mathbf{u}^1, \boldsymbol{\theta}^1, \mathbf{f}^0), \\ &\approx \mathbb{E}_p(\{\mathbf{f}^\ell\}_{\ell=3}^L | \tilde{\mathbf{f}}^2, \{\mathbf{u}^\ell, \boldsymbol{\theta}^\ell\}_{\ell=3}^L) \left[\log p(\mathbf{y} | \mathbf{f}^L) \right], \tilde{\mathbf{f}}^2 \sim p(\mathbf{f}^2 | \mathbf{u}^2, \boldsymbol{\theta}^2, \tilde{\mathbf{f}}^1), \\ &\approx \dots \\ &\approx \mathbb{E}_p(\mathbf{f}^L | \tilde{\mathbf{f}}^{L-1}, \mathbf{u}^L, \boldsymbol{\theta}^L) \left[\log p(\mathbf{y} | \mathbf{f}^L) \right], \tilde{\mathbf{f}}^{L-1} \sim p(\mathbf{f}^{L-1} | \mathbf{u}^{L-1}, \boldsymbol{\theta}^{L-1}, \tilde{\mathbf{f}}^{L-2}), \\ &= \sum_{j=1}^N \mathbb{E}_p(f_j^L | \tilde{f}_j^{L-1}, \mathbf{u}^L, \boldsymbol{\theta}^L) \left[\log p(y_j | f_j^L) \right] \\ &\approx N \mathbb{E}_p(f_i^L | \tilde{f}_i^{L-1}, \mathbf{u}^L, \boldsymbol{\theta}^L) \left[\log p(y_i | f_i^L) \right], i \sim \text{Uniform}\{1, 2, \dots, N\}. \end{aligned} \quad (16)$$

Because of the layer-wise factorization of the joint likelihood Equation 10, each step of the approximation is unbiased. While it is possible to approximate the last-layer expectation with a Monte Carlo sample \tilde{f}_j^L , the expectation is tractable when $y_j | f_j^L$ is a Gaussian or Poisson distribution, or is computable with one-dimensional quadrature (Hensman et al., 2015b).

B. Additional Results

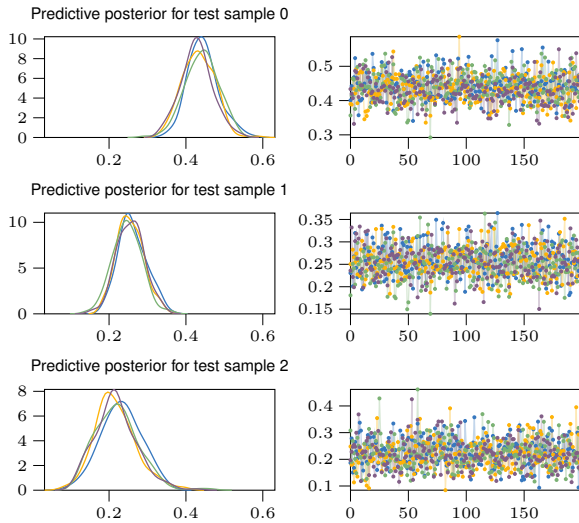


Figure 9: Traces for three test points (4 chains/200 samples).

Table 5: Datasets used, including number of datapoints and their dimensionality.

NAME	N.	D-IN	D-OUT
BOSTON	506	13	1
CONCRETE	1,030	8	1
ENERGY	768	8	2
KIN8NM	8,192	8	1
NAVAL	11,934	16	2
POWERPLANT	9,568	4	1
PROTEIN	45,730	9	1
YACHT	308	6	1
AIRLINE	5,934,530	8	2
HIGGS	11,000,000	28	2

Bayesian Sparse Gaussian Processes

Table 6: Tabular version of Figure 6 in the main paper.

DATASET NAME	TEST MNLL							
	BOSTON	CONCRETE	ENERGY	KIN8NM	NAVAL	POWERPLANT	PROTEIN	YACHT
BSGP	2.47 ± 0.16	3.12 ± 0.04	0.97 ± 0.13	-1.12 ± 0.01	-8.22 ± 0.04	2.71 ± 0.02	2.78 ± 0.01	-0.23 ± 0.13
BSGP 2	2.47 ± 0.15	3.04 ± 0.05	0.95 ± 0.16	-1.40 ± 0.01	-8.23 ± 0.04	2.67 ± 0.02	2.63 ± 0.02	-0.72 ± 0.15
BSGP 3	2.47 ± 0.14	2.96 ± 0.10	0.95 ± 0.15	-1.41 ± 0.01	-8.02 ± 0.04	2.66 ± 0.03	2.57 ± 0.03	-0.83 ± 0.10
BSGP 4	2.48 ± 0.14	2.97 ± 0.06	0.92 ± 0.14	-1.43 ± 0.02	-8.03 ± 0.05	2.65 ± 0.05	2.50 ± 0.03	-0.76 ± 0.13
BSGP 5	2.48 ± 0.12	2.91 ± 0.08	0.75 ± 0.30	-1.43 ± 0.01	-8.09 ± 0.05	2.65 ± 0.03	2.43 ± 0.03	-0.74 ± 0.08
IPVI GP	2.84 ± 0.36	3.19 ± 0.11	1.27 ± 0.07	-1.12 ± 0.02	-5.96 ± 0.89	2.79 ± 0.03	2.81 ± 0.02	1.21 ± 1.50
IPVI GP 2	2.73 ± 0.35	3.13 ± 0.11	1.31 ± 0.28	-1.34 ± 0.02	-4.98 ± 0.48	2.76 ± 0.07	2.65 ± 0.02	0.74 ± 1.13
IPVI GP 3	2.61 ± 0.25	3.08 ± 0.13	1.21 ± 0.12	-1.33 ± 0.03	-4.86 ± 0.23	2.72 ± 0.06	2.74 ± 0.05	1.05 ± 1.77
IPVI GP 4	2.64 ± 0.44	3.11 ± 0.18	1.19 ± 0.25	-1.33 ± 0.01	-4.94 ± 0.20	2.76 ± 0.02	2.79 ± 0.01	2.47 ± 2.34
IPVI GP 5	2.51 ± 0.20	3.08 ± 0.17	1.15 ± 0.22	-1.29 ± 0.02	-5.09 ± 0.49	2.72 ± 0.04	2.80 ± 0.01	2.84 ± 3.64
SGHMC GP	2.82 ± 0.33	3.13 ± 0.09	1.08 ± 0.28	-1.08 ± 0.01	-6.23 ± 0.14	2.76 ± 0.05	2.81 ± 0.01	-0.11 ± 0.28
SGHMC GP 2	2.77 ± 0.37	2.99 ± 0.07	0.91 ± 0.15	-1.32 ± 0.01	-6.57 ± 0.11	2.72 ± 0.04	2.71 ± 0.02	-0.52 ± 0.14
SGHMC GP 3	2.78 ± 0.28	3.02 ± 0.16	0.91 ± 0.14	-1.37 ± 0.02	-6.56 ± 0.09	2.68 ± 0.02	2.66 ± 0.03	-0.57 ± 0.19
SGHMC GP 4	2.75 ± 0.34	2.98 ± 0.13	0.69 ± 0.22	-1.38 ± 0.02	-6.42 ± 0.08	2.67 ± 0.04	2.62 ± 0.02	-0.69 ± 0.12
SGHMC GP 5	3.75 ± 1.91	3.11 ± 0.21	1.00 ± 0.42	-1.39 ± 0.02	-6.55 ± 0.09	2.65 ± 0.04	2.59 ± 0.02	-0.53 ± 0.18
SVGP	2.53 ± 0.25	3.18 ± 0.05	1.75 ± 0.06	-1.01 ± 0.01	-6.67 ± 0.09	2.79 ± 0.02	2.92 ± 0.01	0.78 ± 0.13

Table 7: Tabular version of Figure 7 in the main paper.

DATASET PRIOR TYPE	TEST MNLL							
	BOSTON	CONCRETE	ENERGY	KIN8NM	NAVAL	POWERPLANT	PROTEIN	YACHT
DETERMINANTAL	2.59 ± 0.06	3.30 ± 0.15	1.28 ± 0.10	-1.08 ± 0.01	-7.93 ± 0.32	2.73 ± 0.02	2.79 ± 0.01	0.78 ± 0.21
NORMAL	2.54 ± 0.07	3.12 ± 0.04	0.95 ± 0.08	-1.13 ± 0.01	-8.38 ± 0.05	2.70 ± 0.02	2.77 ± 0.01	-0.32 ± 0.14
STRAUSS	2.67 ± 0.24	3.20 ± 0.05	1.06 ± 0.11	-1.09 ± 0.02	-8.10 ± 0.68	2.74 ± 0.03	2.80 ± 0.01	0.11 ± 0.07
UNIFORM	2.65 ± 0.23	3.21 ± 0.04	1.04 ± 0.07	-1.09 ± 0.01	-8.47 ± 0.04	2.73 ± 0.03	2.79 ± 0.01	0.21 ± 0.09